JCI The Journal of Clinical Investigation

Inhibiting glycolytic metabolism enhances CD8+ T cell memory and antitumor function

Madhusudhanan Sukumar, … , Nicholas P. Restifo, Luca Gattinoni

J Clin Invest. 2013;123(10):4479-4488. https://doi.org/10.1172/JCI69589.

Research Article Oncology

Naive CD8+ T cells rely upon oxidation of fatty acids as a primary source of energy. After antigen encounter, T cells shift to a glycolytic metabolism to sustain effector function. It is unclear, however, whether changes in glucose metabolism ultimately influence the ability of activated T cells to become long-lived memory cells. We used a fluorescent glucose analog, 2-NBDG, to quantify glucose uptake in activated CD8+ T cells. We found that cells exhibiting limited glucose incorporation had a molecular profile characteristic of memory precursor cells and an increased capacity to enter the memory pool compared with cells taking up high amounts of glucose. Accordingly, enforcing glycolytic metabolism by overexpressing the glycolytic enzyme phosphoglycerate mutase-1 severely impaired the ability of CD8+ T cells to form long-term memory. Conversely, activation of CD8+ T cells in the presence of an inhibitor of glycolysis, 2-deoxyglucose, enhanced the generation of memory cells and antitumor functionality. Our data indicate that augmenting glycolytic flux drives CD8+ T cells toward a terminally differentiated state, while its inhibition preserves the formation of long-lived memory CD8+ T cells. These results have important implications for improving the efficacy of T cell–based therapies against chronic infectious diseases and cancer.

Inhibiting glycolytic metabolism enhances CD8+ T cell memory and antitumor function

Madhusudhanan Sukumar,[1] Jie Liu,[2] Yun Ji,[3] Murugan Subramanian,[4] Joseph G. Crompton,[1] Zhiya Yu,[1] Rahul Roychoudhuri,[1] Douglas C. Palmer,[1] Pawel Muranski,[1] Edward D. Karoly,[5] Robert P. Mohney,[5] Christopher A. Klebanoff,[1,6] Ashish Lal,[4] Toren Finkel,[2] Nicholas P. Restifo,[1] and Luca Gattinoni[3]

[1]Center for Cancer Research, Surgery Branch, National Cancer Institute, [2]Center for Molecular Medicine, National Heart, Lung, and Blood Institute, [3]Center for Cancer Research, Experimental Transplantation and Immunology Branch, National Cancer Institute, and [4]Center for Molecular Genetics, NIH, Bethesda, Maryland, USA. [5]Metabolon Incorporated, Durham, North Carolina, USA. [6]Clinical Investigator Development Program, National Cancer Institute, NIH, Bethesda, Maryland, USA.

Naive CD8+ T cells rely upon oxidation of fatty acids as a primary source of energy. After antigen encounter, T cells shift to a glycolytic metabolism to sustain effector function. It is unclear, however, whether changes in glucose metabolism ultimately influence the ability of activated T cells to become long-lived memory cells. We used a fluorescent glucose analog, 2-NBDG, to quantify glucose uptake in activated CD8+ T cells. We found that cells exhibiting limited glucose incorporation had a molecular profile characteristic of memory precursor cells and an increased capacity to enter the memory pool compared with cells taking up high amounts of glucose. Accordingly, enforcing glycolytic metabolism by overexpressing the glycolytic enzyme phosphoglycerate mutase-1 severely impaired the ability of CD8+ T cells to form long-term memory. Conversely, activation of CD8+ T cells in the presence of an inhibitor of glycolysis, 2-deoxyglucose, enhanced the generation of memory cells and antitumor functionality. Our data indicate that augmenting glycolytic flux drives CD8+ T cells toward a terminally differentiated state, while its inhibition preserves the formation of long-lived memory CD8+ T cells. These results have important implications for improving the efficacy of T cell–based therapies against chronic infectious diseases and cancer.

Introduction

CD8+ T cells play an important role in the adaptive immune response to intracellular pathogens and cancer (1, 2). After stimulation with cognate antigen, CD8+ naive T cells (Tns) clonally expand and differentiate into effector T cells (Teffs) and distinct memory T cell subsets, including stem cell memory T cells (Tscms), central memory T cells (Tcms), and effector memory T cells (Tems) (3). These subsets can be identified by distinct cell surface marker expression and gene expression profiles that enable their functional specialization (3). Preclinical studies using adoptive transfer of purified CD8+ T cell populations have revealed that less-differentiated Tscms and Tcms can mediate enhanced antitumor (4, 5) and antiviral (6) responses compared with more-differentiated Tems and Teffs, due to increased proliferative and survival capacities. Thus, there has been considerable interest in understanding the molecular mechanisms governing the formation of long-lived memory T cell subsets to enable the development of more potent immunotherapies against cancer and infectious diseases (3, 7, 8).

Recent findings have highlighted the importance of cellular metabolism in regulating CD8+ T cell differentiation and memory formation (9–12). Metabolic profiling and functional analyses have shown that Tns rely on oxidation of fatty acids (FAO) as a primary source of energy (11, 13, 14). After antigen encounter, however, T cells shift to glycolytic metabolism to sustain effector function (15–18). Similar to Tns, memory CD8+ T cells use FAO to meet their energy demands (19, 20). For instance, CD8+ T cells deficient in TNF receptor–associated factor 6 (Traf6) exhibit defective FAO and fail to form physiological numbers of memory T cells after infection (21). Conversely, enforcing FAO either by overexpressing carnitine palmitoyltransferase 1a (Cpt1a), a rate-limiting enzyme in FAO (22), or by inhibiting activity of the mammalian target of rapamycin (mTOR) resulted in increased numbers of memory CD8+ T cells (21, 23). However, it remains unclear whether immunological memory is regulated by metabolic pathways other than FAO.

Here, we show that induction of high glycolytic activity in CD8+ T cells severely compromises the generation of long-lived memory cells by driving T cells toward a terminally differentiated state. We found that CD8+ T cells taking up high amounts of glucose had a molecular profile characteristic of short-lived effectors and failed to survive upon adoptive transfer. Consistent with these findings, skewing cellular metabolism toward glycolysis by overexpressing the glycolytic enzyme phosphoglycerate mutase-1 (Pgam1) impaired the ability of CD8+ T cells to form long-term memory. Conversely, experiments using the glucose analog 2-deoxyglucose (2DG), an inhibitor of hexokinase-2 (Hk2), indicated that limiting glycolysis in CD8+ T cells favors the establishment of immunological memory. Most importantly, treatment of tumor-specific CD8+ T cells with 2DG enhanced their capacity to trigger the destruction of established tumors. Direct blockade of glycolysis using 2DG was associated with enhanced expression and activity of transcription factors regulating memory versus effector differentiation in CD8+ T cells, providing a link between metabolism and transcriptional regulation of cell fate determination.

Authorship note: Nicholas P. Restifo and Luca Gattinoni contributed equally to this work.

Conflict of interest: Edward D. Karoly and Robert P. Mohney are employees and shareholders of Metabolon Incorporated.

Citation for this article: *J Clin Invest.* 2013;123(10):4479–4488. doi:10.1172/JCI69589.

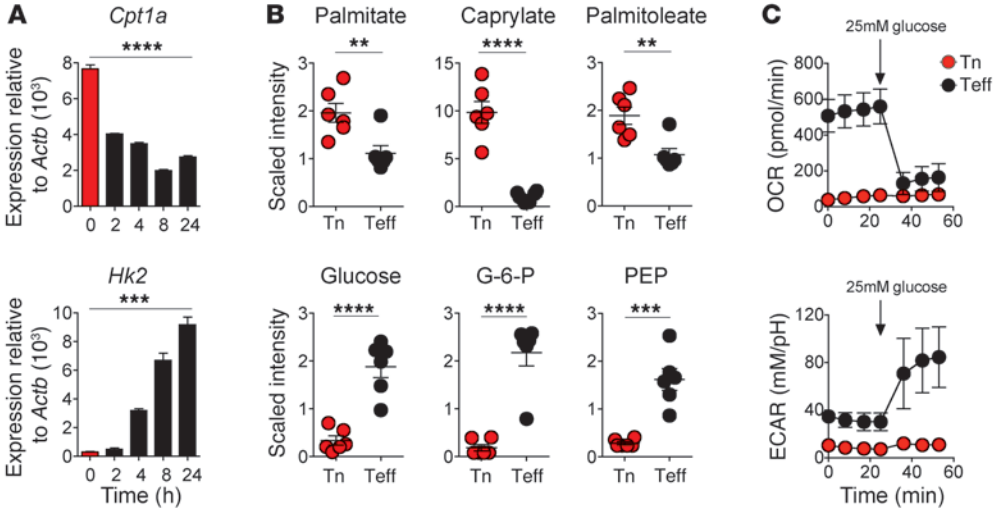

Figure 1

CD8⁺ T cells undergo metabolic reprogramming upon activation and differentiation. (**A**) Quantitative RT-PCR analysis of *Cpt1a* and *Hk2* expression in pmel-1 CD8⁺ T cells at the indicated times after T cell stimulation. Results are presented relative to *Actb*. Data are mean ± SEM of 3 measurements. (**B**) Relative abundance of key metabolites involved in FAO and glycolysis in pmel-1 CD8⁺ Tn and Teff subsets. Data are mean ± SEM of 6 independently generated samples. G-6-P, glucose 6 phosphate; PEP, phosphoenolpyruvate. (**C**) OCR and ECAR of pmel-1 CD8⁺ Tns and Teffs. Data are mean ± SEM of 4 measurements. $^{**}P < 0.01$, $^{***}P < 0.001$, $^{****}P < 0.0001$, 2-tailed Student's *t* test. Results in **A** and **C** are representative of 3 independent experiments.

Results

Metabolic reprogramming upon CD8⁺ T cell differentiation. Activation of CD8⁺ T cells is accompanied by effector differentiation and the loss of memory potential in the majority of cells. To explore the metabolic changes that occur during this process, we first evaluated the gene expression of key rate-limiting enzymes involved in FAO and glycolysis, such as *Cpt1a* and *Hk2*, in Tns after stimulation with antibodies specific to CD3 and CD28. Tns displayed high amounts of *Cpt1a*, but these levels rapidly declined within hours of activation (Figure 1A). In sharp contrast, *Hk2* was profoundly upregulated after anti-CD3/CD28 stimulation (Figure 1A). In addition, numerous other genes regulating glucose metabolism, including several glycolytic enzymes and the glucose and lactate/pyruvate transporters, were increased upon activation and effector differentiation (Supplemental Figure 1; supplemental material available online with this article; doi:10.1172/JCI69589DS1).

To determine whether these changes in gene expression were associated with modifications of cellular metabolism, we evaluated the metabolome of Tns and Teffs using a variety of platforms, including gas chromatography–mass spectrometry (GC/MS) with electron ionization (EI) and liquid chromatography–mass spectrometry/mass spectrometry (LC/MS/MS) with and without EI. Consistent with our gene expression data, metabolomic analysis revealed that Teffs had increased amounts of glycolytic metabolites, but low quantities of medium- and long-chain fatty acids (the principal substrates for FAO), compared with Tns (Figure 1B). To assess whether these steady-state changes in metabolites reflected functional differences in Tn and Teff metabolism, we measured the metabolic changes occurring in response to glucose supplementation. We evaluated the extracellular acidification rate (ECAR), which quantifies proton production as a surrogate for lactate production, and thus reflects overall glycolytic flux, and the oxygen consumption rate (OCR), a measure of mitochondrial respiration. Consistent with previous findings (18), Teffs exhibited increased metabolic activity compared with Tns, as revealed by basal OCR and ECAR measurements (Figure 1C). However, Tns relied on preferential use of oxidative phosphorylation (OXPHOS) to meet their energy demands (Supplemental Figure 2). After glucose supplementation, Teffs promptly engaged glycolysis, as manifested by a sharp increase in ECAR levels accompanied by a rapid reduction in OCR (Figure 1C). Thus, we observed metabolic reprogramming from lipid oxidation to glycolysis to be one of the early metabolic switches during CD8⁺ T cell activation and differentiation, a finding consistent with recent observations in CD4⁺ T cells (17).

Glucose uptake segregates short-lived Teffs from memory T cell precursors. Although these data indicated that activation and effector differentiation of CD8⁺ T cells was associated with dramatic increases in glycolysis and lactate production, it remained to be determined whether these changes in glucose metabolism could ultimately influence the ability of activated T cells to become long-lived memory cells. To separate activated CD8⁺ T cells based on intrinsic differences in glycolytic activities, we used a fluorescent glucose analog, 2-(N-[7-nitrobenz-2-oxa-1,3-diazol-4-yl]amino)-2-deoxyglucose (2-NBDG), which allows for direct quantification of glucose incorporation in living cells by flow cytometry (24, 25). We stimulated pmel-1 splenocytes with cognate antigen gp100 and IL-2 to induce effector differentiation (26) and isolated T cells with low and high 2-NBDG uptake (2-NBDG^{lo} and 2-NBDG^{hi}, respectively) by flow cytometry sorting (Figure 2A). Uptake of radiolabeled 2DG confirmed that 2-NBDG uptake discriminated cells based on their capacity to incorporate glucose (Figure 2B). 2-NBDG^{hi} T cells had increased mRNA levels of solute carrier family 2 (*Slc2a1*; which encodes the glucose transporter Glut-1) and *Hk2* compared with 2-NBDG^{lo} cells (Supplemental Figure 3), which suggests that this fluorescent glucose analog could efficiently distinguish cells with differential glucose metabolism. Furthermore, cells labeling intensely with 2-NBDG displayed greater ECAR than did their 2-NBDG^{lo} counterparts (Figure 2C), which indicates that differential 2-NBDG uptake reflects functional differences in glycolytic metabolism. Interestingly, 2-NBDG^{lo} T cells displayed a higher OCR/ECAR ratio (Figure 2D), which suggests that these cells preferentially used OXPHOS compared with 2-NBDG^{hi} cells. However, this difference in OCR/ECAR ratio was driven by the denominator, as basal OCR was lower in 2-NBDG^{lo} cells (Supplemental Figure 4A). These functional studies indicated that 2-NBDG^{hi} cells have increased energetic demand compared

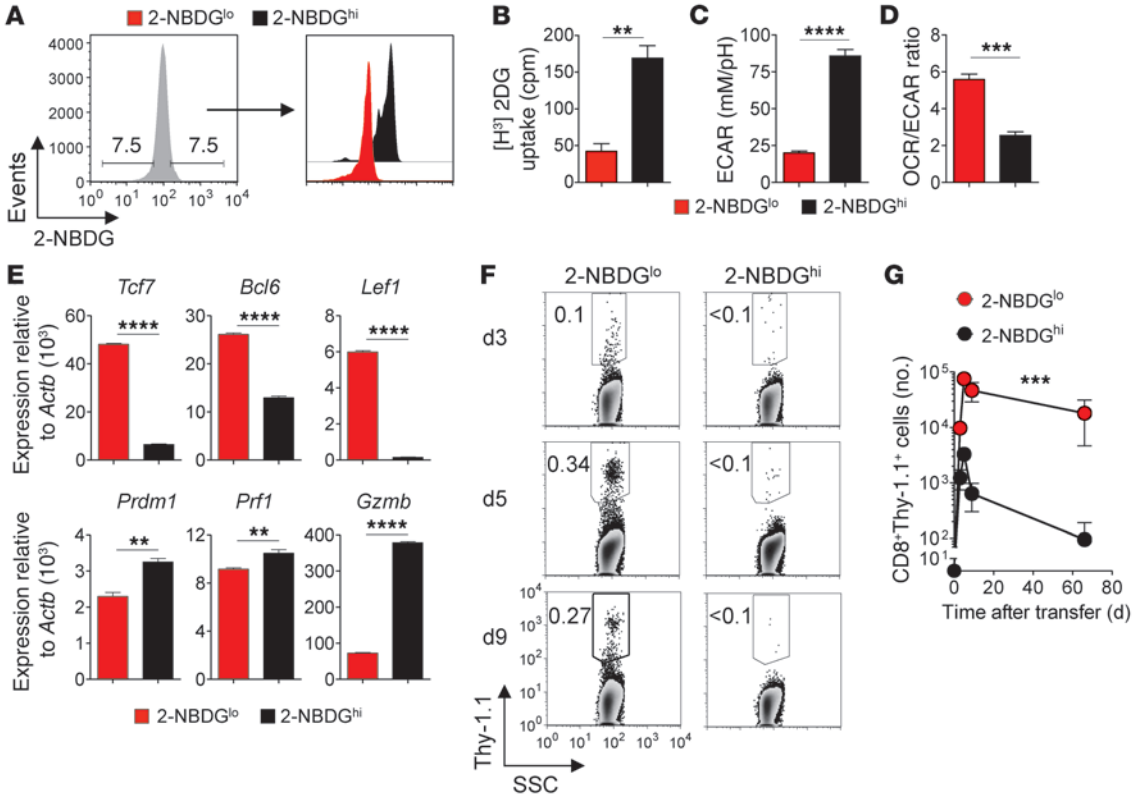

Figure 2

Glucose uptake segregates short-lived Teffs from memory T cell precursors. (**A**–**D**) Flow cytometry sort (**A**), 2DG uptake (**B**), ECAR (**C**), OCR/ECAR ratio (**D**),and quantitative RT-PCR analysis of key memory and effector genes (**E**) in 2-NBDG^{lo} and 2-NBDG^{hi} Teffs. Data are mean ± SEM of 4 (**B**–**D**) or 3 (**E**) measurements. Results in **E** are presented relative to *Actb*. (**F** and **G**) Flow cytometry analysis (**F**) and numbers (**G**) of CD8$^+$ Thy-1.1$^+$ T cells on the indicated days after adoptive transfer of 2 × 10^5 2-NBDG^{hi} and 2-NBDG^{lo} cells into wild-type mice and subsequent infection with gp100-VV. Density plots in **F** are shown after gating on CD8$^+$ cells. Numbers represent percent cells in the respective gates. Data in **G** are mean ± SEM of 3–6 samples. $^{**}P < 0.01$, $^{***}P < 0.001$, $^{****}P < 0.0001$, 2-tailed Student's *t* test (**B**–**E**) or 2-way ANOVA (**G**). Data are representative of 5 (**A**), 3 (**E**), or 2 (**B**–**D**, **F**, and **G**) independent experiments.

with 2-NBDG^{lo} cells, which appear more metabolically quiescent. Accordingly, forward scatter (FSC) and side scatter (SSC) measurements of these 2 populations revealed that 2-NBDG^{hi} cells were blastic and highly granular, whereas 2-NBDG^{lo} cells appeared smaller in size (Supplemental Figure 4B). Notably, these metabolic differences were not merely due to lack of proper Tn stimulation. Indeed, dilution of the cell proliferation dye eFluor670 and measurement of the T cell activation markers CD44, CD25, and CD69 revealed that 2-NBDG^{lo} cells had undergone extensive proliferation and activation after priming (Supplemental Figure 5).

To evaluate whether differences in glucose metabolism in CD8$^+$ T cells are associated with differences in transcriptional regulation of T cell differentiation, we quantified the mRNA levels of key transcription factors and molecules associated with either memory precursors or short-lived, terminally differentiated Teffs in 2-NBDG^{hi} and 2-NBDG^{lo} cells (8). We found that the Wnt–β-catenin signaling transducers transcription factor 7 (*Tcf7*), lymphoid enhancer factor 1 (*Lef1*), and B cell CLL/lymphoma 6 (*Bcl6*), which promote memory CD8$^+$ T cell formation (4, 27–29), were significantly overexpressed in 2-NBDG^{lo} versus 2-NBDG^{hi} CD8$^+$ T cells (Figure 2E). In contrast, PR domain containing 1, with ZNF domain (*Prdm1*) — which encodes B lymphocyte–induced maturation protein-1 (Blimp-1), a master regulator of terminal differentiation (30–33) — was enriched in 2-NBDG^{hi} cells compared with their 2-NBDG^{lo} counterparts (Figure 2E). In addition, perforin (*Prf1*) and granzyme B (*Gzmb*), which encode key cytotoxic effector molecules, were also highly expressed in 2-NBDG^{hi} cells (Figure 2E). Thus, glucose uptake enabled the segregation of T cells that had molecular profiles associated with Teffs (2-NBDG^{hi}) and memory precursor cells (2-NBDG^{lo}).

Given these findings, we sought to ascertain whether glucose uptake could also be used to segregate T cells with differential capacity to establish memory in vivo. We adoptively transferred 2-NBDG^{hi} and 2-NBDG^{lo} cells into wild-type mice, which were then infected with a recombinant strain of vaccinia virus encoding the cognate antigen gp100 (referred to herein as gp100-VV). Strikingly, cells that experienced an increased rate of glucose metabolism exhibited poor engraftment, proliferation, and survival capacities compared with 2-NBDG^{lo} cells, which exhibited 10- to 100-fold higher frequency over the time course of infection (Figure 2, F and G). Taken together, these findings indicated that during T cell activation, there is heterogeneous induction of glycolysis: cells that uptake high levels of glucose becoming short-lived Teffs, whereas cells that maintain reduced glucose incorporation preferentially form memory.

Constitutive activation of glycolytic flux limits CD8$^+$ T cell memory development. To determine whether high glycolytic flux is merely

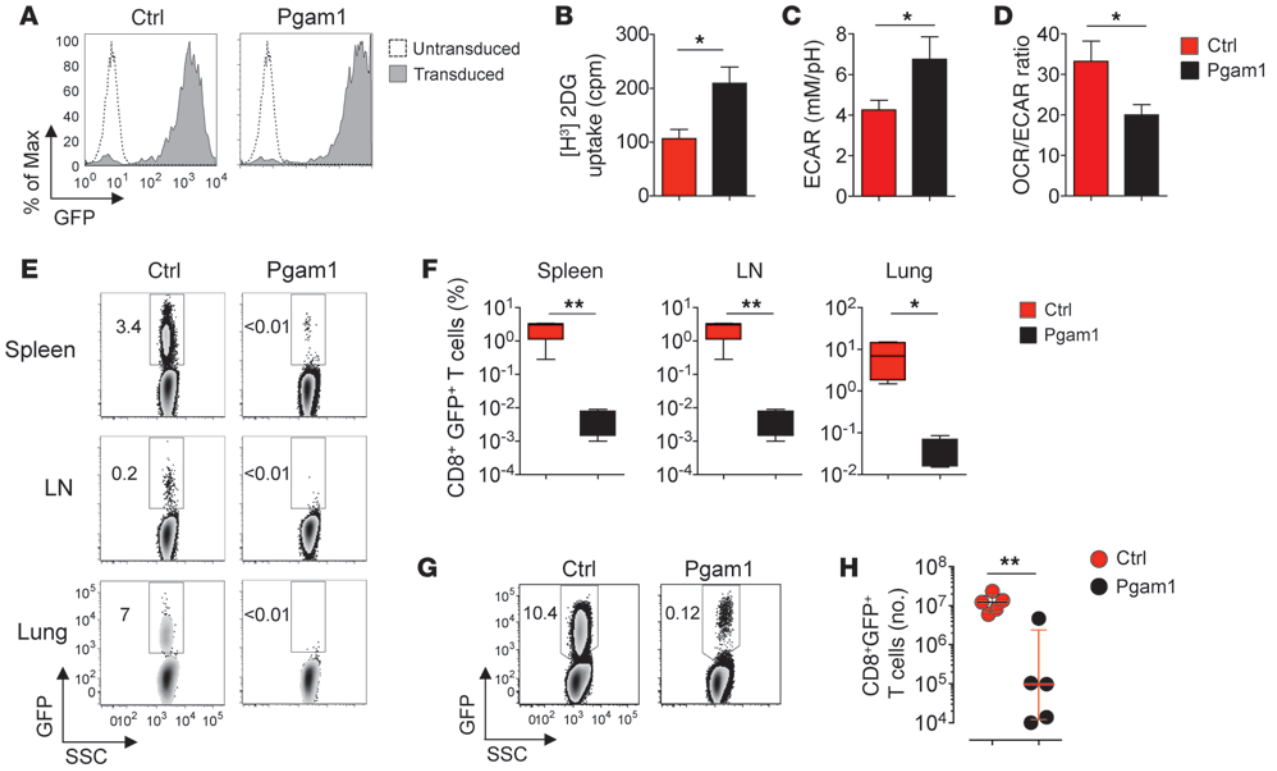

Figure 3

Enforced glycolytic flux limits long-term survival of CD8⁺ T cells. (**A**) Flow cytometry post-sort analysis of GFP expression in pmel-1 CD8⁺ T cells transduced with a retrovirus encoding empty GFP control or Pgam1 GFP. (**B**) Radiolabeled 2DG uptake in control and Pgam1-transduced CD8⁺ T cells. (**C** and **D**) ECAR (**C**) and OCR/ECAR ratio (**D**) of control and Pgam1-transduced CD8⁺ T cells. Data are mean ± SEM of 4 measurements. (**E** and **F**) Flow cytometry analysis (**E**) and frequency (**F**) of CD8⁺GFP⁺ T cells 30 days after adoptive transfer of 1 × 10^5 control and Pgam1-transduced CD8⁺ T cells into wild-type mice and subsequent infection with gp100-VV. Density plots in **E** are shown after gating on CD8⁺ cells. Numbers represent percent cells in the GFP⁺ gate. Data in **E** are mean ± SEM of 3 samples. (**G** and **H**) Flow cytometry analysis (**G**) and number (**H**) of CD8⁺GFP⁺ T cells in mice as in **E** and **F**, 5 days after heterologous vaccination with ad-gp100. Density plots in **G** are shown after gating on CD8⁺ cells. Numbers represent percent cells in the GFP⁺ gate. *$P < 0.05$, **$P < 0.01$, 1-tailed (**C** and **D**) or 2-tailed (**B**, **F**, and **H**) Student's *t* test. Data are representative of 5 (**A**) or 2 (**B**–**H**) independent experiments.

associated with cells with an impaired capacity to become memory or, rather, is causally related to the observed defect in CD8⁺ T cell memory formation, we used a genetic approach to enforce glycolytic metabolism. We transduced CD8⁺ T cells with the glycolytic enzyme Pgam1, which has been shown to enhance glycolytic flux (34, 35) and modulate the cellular lifespan of primary mouse embryonic fibroblasts (35). *Pgam1*-overexpressing cells were isolated based on the expression of the reporter marker GFP and compared with control cells engineered to express GFP alone (Figure 3A). Enforced expression of Pgam1 induced CD8⁺ T cells to adopt a predominantly glycolytic phenotype, as revealed by augmented uptake of radiolabeled 2DG, increased ECAR levels, and lower OCR/ECAR ratio compared with controls (Figure 3, B–D). To explore whether ectopic expression of Pgam1 influences CD8⁺ T cell differentiation in vivo, we adoptively transferred *Pgam1*-overexpressing pmel-1 CD8⁺ T cells into wild-type mice and monitored the expansion and long-term persistence of antigen-specific T cells after gp100-VV infection. At the peak of the immune response, the frequency of *Pgam1*-transduced T cells in the spleen was significantly reduced, but no major phenotypic differences were observed compared with controls (Supplemental Figure 6), which indicates that the high glycolytic activity mainly impaired T cell engraftment and expansion in vivo. Strikingly, at 1 month after transfer, these differences in frequency became more pronounced, as *Pgam1*-transduced T cells had decreased long-term survival in both lymphoid and peripheral tissues (Figure 3, E and F). To determine whether enforced glycolysis affects the ability of memory T cells to respond to antigen reexposure, at 30 days after primary infection with gp100-VV, we challenged the hosts with a heterologous adenovirus type 2 encoding gp100 antigen (referred to herein as ad-gp100) and evaluated the proliferative responses of transduced T cells at the peak of the immune response. We found that secondary progeny of *Pgam1*-transduced T cells were severely impaired, with a 100-fold reduction in frequency and absolute numbers (Figure 3, G and H). Taken together, these findings using enforced overexpression of a key glycolytic enzyme were consistent with the view that acquisition of a high glycolytic metabolism severely limits the formation of CD8⁺ T cell memory in vivo.

Inhibition of glycolysis enhances memory CD8⁺ T cell formation. Our experiments using adoptive transfer of CD8⁺ T cells with intrinsic differences in glucose metabolism and studies using a genetic approach to augment glycolytic function indicated that CD8⁺ T cells displaying higher glycolytic flux had a limited capacity to establish immunological memory. It remained to be addressed,

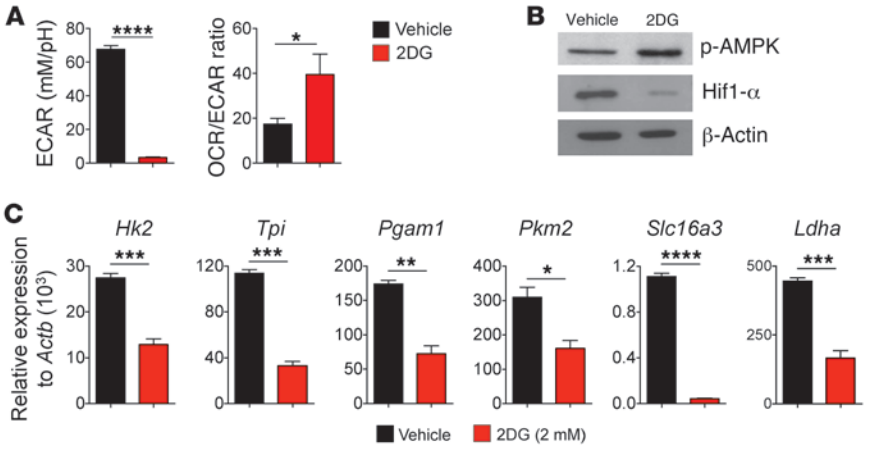

Figure 4

Inhibition of glycolysis triggers activation of energy stress signaling, which reinforces glycolysis shutdown. (**A**) ECAR and OCR/ECAR ratio of CD8⁺ T cells activated by antibodies specific to CD3 and CD28 in the presence of 2DG (2 mM) or DMSO vehicle. Data are mean ± SEM of 4 measurements. (**B**) Immunoblot analysis of p-AMPK and Hif1-α protein in cells as in **A**. β-actin was used as a loading control. (**C**) Quantitative RT-PCR analysis of the expression of glycolytic enzymes in CD8⁺ T cells. Results are presented relative to *Actb*. *Tpi*, triose phosphate isomerase; *Pkm2*, pyruvate kinase muscle; *Slc16a3*, solute carrier family 16, member 3; *Ldha*, lactate dehydrogenase A. Data are mean ± SEM of 3 measurements. $^{*}P < 0.05$, $^{**}P < 0.01$, $^{***}P < 0.001$, $^{****}P < 0.0001$, 1-tailed (**A**, OCR/ECAR) or 2-tailed (**A**, ECAR, and **C**) Student's *t* test. Data are representative of 3 (**C**) or 2 (**A** and **B**) independent experiments.

however, whether direct inhibition of glycolysis would conversely enhance T cell survival and the capacity to form long-lived memory cells. To directly target the glycolytic pathway in CD8⁺ T cells, we used the Hk2 inhibitor 2DG. Previous reports have demonstrated that cell proliferation was blocked by high concentrations of 2DG (50 mM) (36). However, low doses of 2DG have been used to address the role of glycolysis in directing the fate decision of CD4⁺ Th17 cells versus Foxp3⁺ Tregs (37, 38). Based on these findings and titration experiments (Supplemental Figure 7), we chose a 2-mM dose for the present study. Activation of CD8⁺ T cells in the presence of 2DG was sufficient to inhibit glycolytic flux and dramatically reduce lactate production, as revealed by measurement of ECAR (Figure 4A). Moreover, inhibition of glycolysis induced CD8⁺ T cells to preferentially use OXPHOS as a source of energy, as revealed by a higher OCR/ECAR ratio in 2DG-treated CD8⁺ T cells (Figure 4A), but it did not enhance OXPHOS, as basal OCR was also reduced compared with control cells (Supplemental Figure 8). Consistent with recent findings (39), 2DG treatment triggered the activity of AMPK, as manifested by increased levels of AMPK phosphorylation (Figure 4B). AMPK is a well-established negative regulator of mTOR activity, which is required to sustain glucose uptake and glycolysis in CD8⁺ T cells via induction of the hypoxia-inducible factor 1 (Hif1) transcription factor complex (40). Accordingly, Hif1-α protein levels were decreased in CD8⁺ T cells treated with 2DG (Figure 4B). Finally, the mRNA levels of key enzymes and transporters involved in the glycolytic machinery were also reduced (Figure 4C), which indicates that 2DG not only inhibits glycolysis, but also triggers the activation of starvation signaling, which then reinforces shutdown of the glycolytic machinery at a transcriptional level.

To determine whether manipulating glycolysis during T cell priming modulates CD8⁺ T cell fate, we evaluated the transcriptional program and phenotype of differentiating CD8⁺ T cells. We assessed the expression levels of key transcriptional regulators implicated in memory T cell and Teff formation, such as *Tcf7*, *Lef1*, *Bcl6*, and *Prdm1*, as well as T cell differentiation markers, including CD44, CD62L, CD27, and KLRG-1. 2DG-treated T cells displayed increased mRNA levels of *Bcl6*, *Tcf7*, and *Lef1*, while control cells were enriched in *Prdm1* mRNA (Figure 5A). Additionally, 2DG prevented the induction of effector molecule–encoding genes, such as *Prf1* and *GzmB* (Figure 5A). Thus, gene transcription analysis provided evidence that blockade of glycolysis by 2DG enforces a transcriptional program characteristic of memory cells. Moreover we observed that 2DG-treated T cells retained higher expression of CD62L, a molecule found in Tns and early memory T cell subsets, compared with control cells (Supplemental Figure 9). To test whether inhibition of glycolysis during T cell priming programs CD8⁺ T cells to adopt a diverse fate in vivo, we transferred 2DG-treated pmel-1 CD8⁺ T cells into wild-type mice infected with gp100-VV and evaluated the expansion, persistence, and phenotypic changes of transferred cells. 2DG-treated CD8⁺ T cells expanded robustly, as indicated by increased frequencies and numbers of CD8⁺Thy-1.1⁺ T cells in the spleen at the peak of the immune response compared with control cells ($P < 0.01$; Supplemental Figure 10, A and B). Despite increased expansion, a higher proportion of 2DG-treated cells retained a memory phenotype, whereas the majority of control CD8⁺ T cells underwent terminal differentiation, as revealed by the loss of CD62L and concomitant acquisition of the senescence marker KLRG-1 (Supplemental Figure 10, C and D). These quantitative and qualitative differences between 2DG-treated T cells and controls became more prominent during the memory phase of immune response. We observed 100-fold higher frequencies of pmel-1 CD8⁺ T cells in both lymphoid and nonlymphoid tissues of animals that received adoptive transfer of 2DG-treated versus control T cells (Figure 5, B and C). Notably, the persisting progeny of T cells primed in the presence of 2DG were relatively enriched in Tcms compared with control cells, which preferentially gave rise to senescent KLRG-1⁺ T cells (Figure 5D). Consistent with these findings, recall responses were significantly increased in mice that received adoptive transfer of 2DG-treated T cells (Figure 5, E and F). Together, these findings indicate that specific inhibition of glycolysis during priming enhances not only the quantity, but also the quality, of antigen-specific memory CD8⁺ T cells.

Inhibition of glycolysis sustains Foxo1 activity and enhances lymphoid homing. Recent studies have demonstrated the importance of Foxo1 in regulating memory versus effector lineage commitment in CD8⁺ T cells (20, 41, 42). To determine whether inhibition of glucose metabolism in CD8⁺ T cells regulated Foxo1 activity, we first evaluated Foxo1 phosphorylation in differentiating CD8⁺ T cells stimulated in the presence or absence of 2DG. Stimulation of CD8⁺ T cells induced phosphorylation of Foxo proteins at T24/T36 residues, a process that was prevented by 2DG treatment

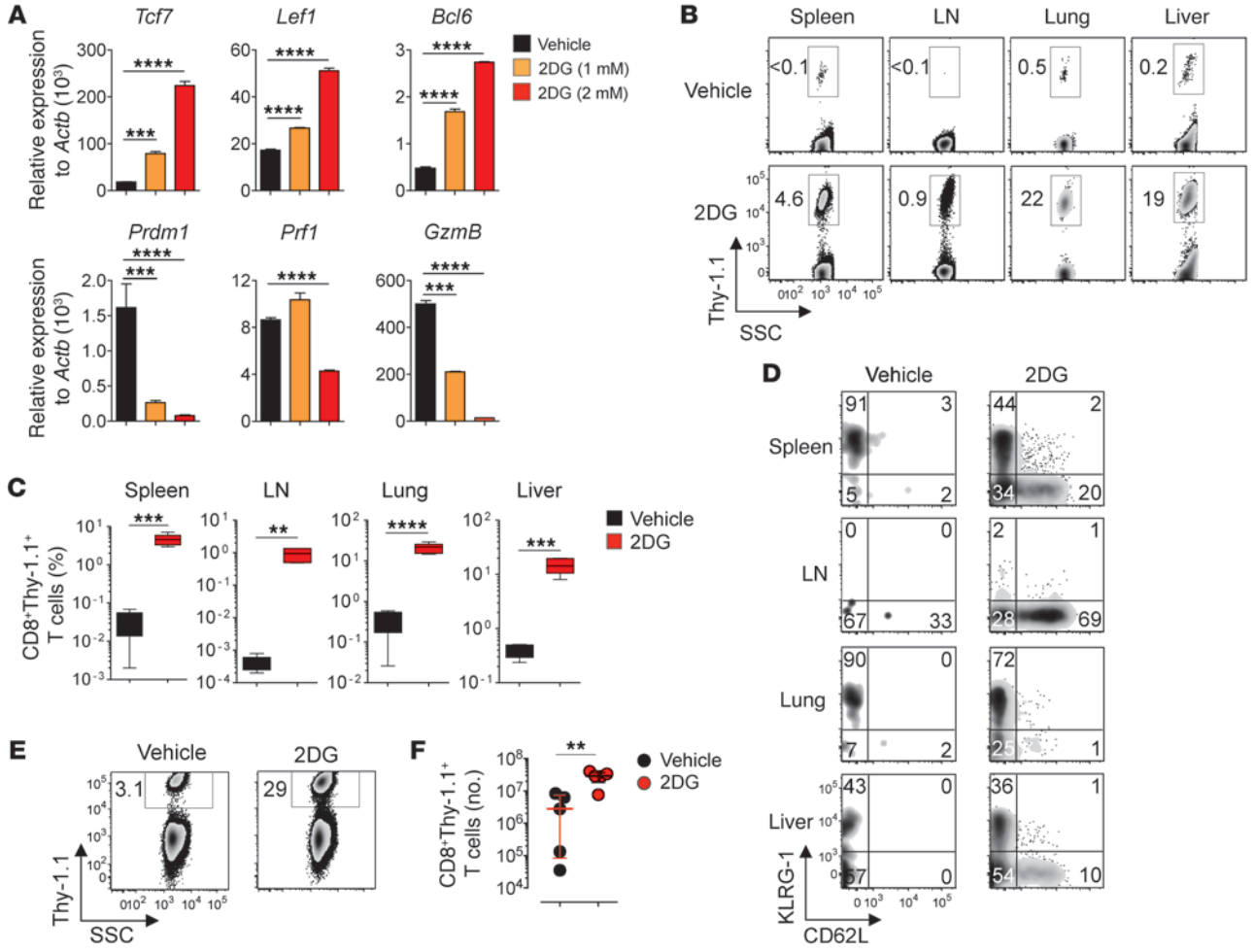

Figure 5

Inhibition of glycolysis enhances memory CD8⁺ T cell formation. (**A**) Quantitative RT-PCR analysis of the expression of key memory and effector genes in pmel-1 CD8⁺ T cells 4 days after activation in the presence of 2DG or vehicle (culture media). Results are presented relative to *Actb*. Data are mean ± SEM of 3 measurements. (**B**–**D**) Flow cytometry analysis (**B** and **D**) and frequency (**C**) of CD8⁺Thy-1.1⁺ T cells 40 days after adoptive transfer of 10^6 pmel-1 CD8⁺Thy-1.1⁺ T cells, generated as in **A**, into wild-type mice and subsequent infection with gp100-VV. Density plots are shown after gating on CD8⁺ (**B**) or CD8⁺Thy-1.1⁺ (**D**) cells. Numbers represent percent cells in the Thy-1.1⁺ gate (**B**) or respective quadrants (**D**). Data in **C** are mean ± SEM of 3–4 samples. (**E** and **F**) Flow cytometry analysis (**E**) and numbers (**F**) of CD8⁺Thy-1.1⁺ T cells in mice treated as in **B**–**D**, 5 days after heterologous vaccination with ad-gp100. Density plots in **E** are shown after gating on CD8⁺ cells. Numbers represent percent cells in the Thy-1.1⁺ gate. $^{**}P < 0.01$, $^{***}P < 0.001$, $^{****}P < 0.0001$, 2-tailed Student's *t* test. Data are representative of 3 (**A**) or 2 (**B**–**F**) independent experiments.

(Figure 6A). Phosphorylation of Foxo1 facilitates its binding to cytosolic 14-3-3 scaffold proteins, which prevents translocation of Foxo1 into the nucleus, thus resulting in a loss of Foxo1 transcriptional activity (42). Consistently, we found that the majority of Foxo1 protein was sequestered into the cytoplasm after CD8⁺ T cell stimulation, while treatment with 2DG promoted Foxo1 nuclear localization (Figure 6B).

To confirm that changes in Foxo1 compartmentalization resulted in differences in Foxo1 transcriptional activity, we measured the expression of Kruppel-like factor 2 (*Klf2*), a well-characterized Foxo1 target gene (43, 44). Quantitative RT-PCR analysis revealed that while control cells displayed low levels of *Klf2* expression, 2DG treatment resulted in a dose-dependent increase in *Klf2* and its target genes, such as selectin L (*Sell*; which encodes CD62L), chemokine (C-C motif) receptor 7 (*Ccr7*), and sphingosine-1-phosphate receptor 1 (*S1p1r*), which control the ability of T cells to home to secondary lymphoid structures (Figure 6C and refs. 44, 45). Finally, to determine whether modulation of glucose metabolism could regulate such lymphoid homing behavior, we adoptively transferred congenically marked control (Thy-1.1⁺) or 2DG-treated (Ly5.1⁺Thy-1.1⁺) cells in the same hosts and evaluated the presence of transferred cells in both lymphoid and peripheral tissues 24 hours later. Strikingly, CD8⁺ T cells treated with 2DG exhibited 10-fold greater migration to lymph nodes compared with control cells, whereas both groups were found at similar frequency in lungs (Figure 6, D and E). Our results indicate that sustained glycolytic activity is required to maintain cell migratory properties characteristic of cytotoxic effector T lymphocytes and that direct blockade of glycolysis reprograms T cells to preferentially migrate to lymphoid tissues.

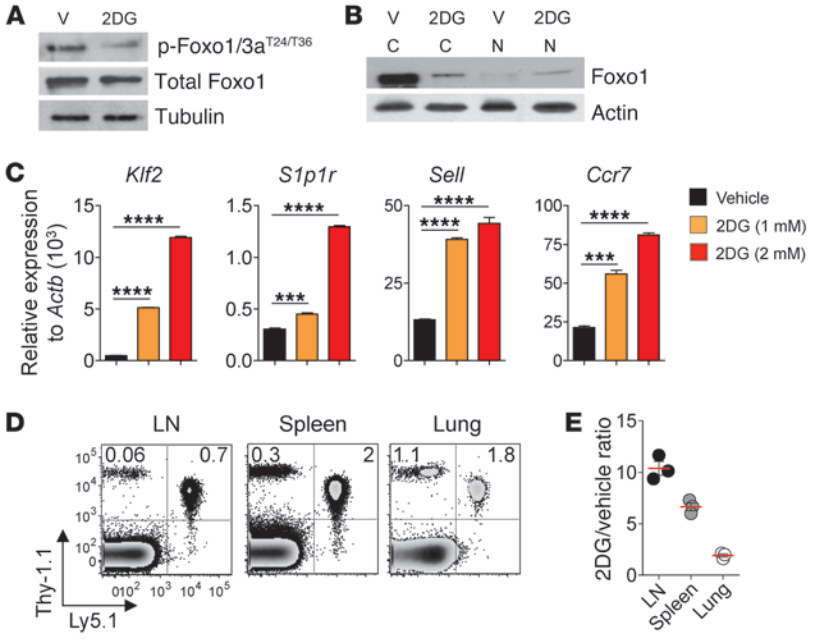

Figure 6

Blockade of glycolysis reprograms CD8⁺ T cell migration. (**A**) Immunoblot analysis of phosphorylated Foxo1/3a proteins in pmel-1 CD8⁺ T cells 4 days after activation in the presence of 2DG or vehicle (culture media). Tubulin was used as a loading control. (**B**) Immunoblot analysis of Foxo1 protein in isolated fractions of CD8⁺ T cells activated for 24 hours in the presence of 2DG or vehicle. β-actin was used as a loading control. (**C**) Quantitative RT-PCR analysis of *Klf2*, *S1p1r*, *Sell*, and *Ccr7* expression in pmel-1 CD8⁺ T cells as in **A**. Results are presented relative to *Actb*. Data are mean ± SEM of 3 measurements. (**D** and **E**) Flow cytometry analysis (**D**) and Ly5.1⁺Thy-1.1⁺/Thy-1.1⁺ ratio (**E**) of CD8⁺ T cells in the lymph nodes, spleen, and lungs 24 hours after adoptive transfer of 1:1 mix of 10^6 Ly5.1⁺Thy-1.1⁺ (2DG-treated) and Thy-1.1⁺ (vehicle) pmel-1 CD8⁺ T cells into wild-type mice. Flow cytometry in **D** is shown after gating on CD8⁺ cells. Numbers represent percent cells in the respective quadrants. Data in **E** are mean ± SEM. ***$P < 0.001$, ****$P < 0.0001$, 2-tailed Student's *t* test. Data are representative of 3 (**C**) or 2 (**A**, **B**, **D**, and **E**) independent experiments.

Glycolysis blockade enhances intratumoral T cell responses and augments antitumor functionality. Studies in both tumor (46, 47) and chronic viral (48) models have demonstrated that CD8⁺ T cells with the capacity to home to secondary lymph nodes, where they can be effectively stimulated by professional antigen-presenting cells, are more effective in adoptive immunotherapy. Furthermore, the ability of T cells to robustly proliferate and persist in the long term after transfer has been correlated with effective antitumor responses in mice and humans receiving adoptive T cell–based therapies (4, 5, 49–51). Thus, we hypothesized that tumor treatment could be improved by inhibiting glycolytic metabolism in tumor-specific T cells during ex vivo expansion. pmel-1 CD8⁺ T cells were primed with cognate gp100 peptide antigen, in the presence or absence of 2DG, and adoptively transferred into wild-type mice bearing large vascularized B16 melanoma tumors. At 3 days after transfer, tumor-specific T cells infiltrated the tumor bed at similar levels (Figure 7A), which indicates that inhibition of glycolysis during priming did not affect initial trafficking to tumors. However, with time, 2DG-treated cells more efficiently accumulated within the tumors (Figure 7A). Notably, within the tumors, T cells primed in the presence of 2DG acquired glycolytic ability, as manifested by the high expression of key glycolytic enzymes (Figure 7B). Consistent with a recent report indicating that glycolysis facilitates full effector functions (18), 2DG-treated cells exhibited increased production of IFN-γ and TNF-α compared with control cells after adoptive transfer (Figure 7C). Importantly, in vitro 2DG treatment of pmel-1 CD8⁺ T cells significantly augmented their in vivo antitumor activity, resulting in improved tumor regression (Figure 7D). Consequently, mice that received 2DG-treated cells exhibited prolonged survival ($P < 0.01$; Figure 7E). Thus, specific inhibition of glycolysis by 2DG in tumor-specific CD8⁺ T cells promoted the formation of memory CD8⁺ T cells under physiological conditions and augmented their antitumor function in mice bearing large vascularized tumors.

Discussion

Diverse metabolic changes accompany CD8⁺ T cell activation (9, 11). For instance, after antigen stimulation, T cells switch to glycolytic metabolism to sustain effector function (18). Metabolic reprogramming to glycolysis, however, has been found to be dispensable for proliferation or survival of T cells in the short term in vitro studies in the presence of alternative fuel (18). Whether specific changes in glucose metabolism can influence long-term survival of activated T cells and their capacity to enter into the memory pool in vivo remains unknown. In this study, we found that graded levels of glycolysis can act as a metabolic rheostat determining the decision between memory and terminal effector differentiation in CD8⁺ T cells. This conclusion was supported by 3 main lines of evidence. First, activated CD8⁺ T cells sorted on the basis of intrinsic differences in glucose metabolism experienced a divergent fate in vivo: CD8⁺ T cells displaying high glycolytic activity tended to be short-lived, whereas cells with low glycolytic metabolism established memory. Second, enforcing glycolysis by overexpression of Pgam1 severely impaired the ability of CD8⁺ T cells to persist in the long term and form memory in vivo. Finally, specific inhibition of glycolytic flux using 2DG during T cell priming enhanced the ability of CD8⁺ T cells to become long-lived memory cells.

The finding that graded levels of glycolytic flux can act as a metabolic rheostat to regulate CD8⁺ T cell fate determination has parallels in CD4⁺ T cell biology. High levels of glycolytic activity were found in polarizing conditions that sustain effector differentiation among effector cell subsets, such as Th1, Th2, and Th17, but were not observed during the generation of Tregs, which instead displayed elevated rates of lipid oxidation (37, 38). Accordingly, blockade of glycolysis using 2DG inhibited Th17 differentiation, but surprisingly promoted Treg formation (37).

It has recently been established that the formation of memory CD8⁺ T cells can be enhanced by augmenting OXPHOS (11). For instance, overexpression of Cpt1a, a rate-limiting enzyme in FAO, increases memory CD8⁺ T cell numbers (22). It should be pointed out, however, that our results obtained by manipulation of glucose metabolism did not merely result from an enhancement in OXPHOS as a compensatory mechanism in response to

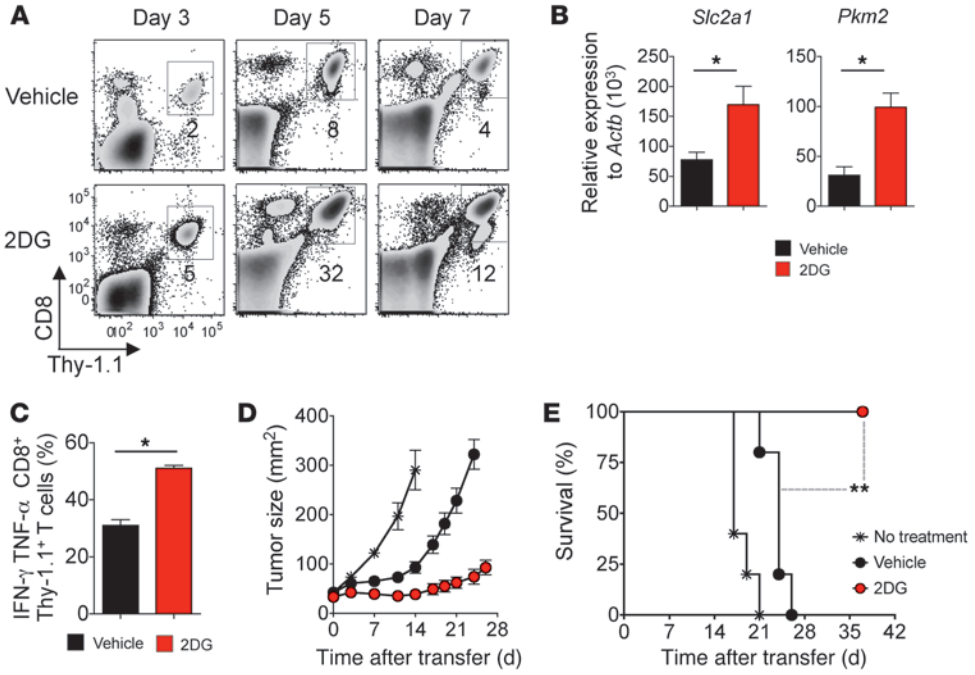

Figure 7

Inhibition of glycolysis during ex vivo expansion enhances the antitumor function of CD8⁺ T cells. (**A**) Flow cytometry analysis of CD8⁺ Thy-1.1⁺ T cells in the tumor at the indicated times after adoptive transfer of 10^6 pmel-1 CD8⁺ Thy-1.1⁺ T cells generated in vitro in the presence of 2DG or vehicle (culture media) into sublethally irradiated B16-tumor bearing mice after gp100-VV vaccination and exogenous IL-2. Numbers represent percent CD8⁺ Thy-1.1⁺ cells. (**B**) Quantitative RT-PCR analysis of *Slc2a1* and *Pkm2* expression in pmel-1 CD8⁺ T cells isolated from tumors 5 days after adoptive transfer as in **A**. Results are presented relative to *Actb*. Data are mean ± SEM of 3 measurements. (**C**) Percent IFN-γ– and TNF-α–producing pmel-1 CD8⁺ Thy-1.1⁺ cells isolated from spleens 5 days after adoptive transfer as in **A**. (**D** and **E**) Tumor size (**D**) and survival (**E**) of sublethally irradiated B16 tumor-bearing mice as in **A**. Data are mean ± SEM of 5 samples. **P* < 0.05, ***P* < 0.01, 2-tailed Student's *t* test (**B** and **C**) or log-rank (Mantel-Cox) test (**E**). Data are representative of 2 independent experiments.

glycolytic shutdown, but were likely dependent on enforcement of cellular quiescence secondary to activation of glucose starvation signaling. Indeed, in all experimental settings used in the present studies, activated CD8⁺ T cells that were prone to form memory exhibited a lower overall bioenergetic profile, characterized not only by reduced levels of ECAR, but also by basal levels of OCR not exceeding those found in highly glycolytic cells.

Consistent with this view, we found that inhibition of glycolysis using 2DG was associated with increased activity of AMPK, an evolutionarily conserved protein kinase that enforces quiescence to limit energy demands in response to energy stress (9). Recently, AMPK has emerged as a key regulator of memory CD8⁺ T cell formation. For example, AMPKα1-deficient T cells were found to have profound defects in their ability to generate memory CD8⁺ T cell responses during *Listeria monocytogenes* infection (39), whereas pharmacologic activation of AMPK with metformin resulted in enhanced CD8⁺ T cell memory (21).

The levels of glycolytic flux appeared to be tightly linked to transcriptional programs regulating CD8⁺ T cell differentiation. Low levels of glycolysis were associated with high expression of transcription factors that promote CD8⁺ T cell memory, such as *Tcf7*, *Lef1*, and *Bcl6*, as well as increased activity of Foxo1, a key transcription factor that regulates memory T cell differentiation and the migratory pattern characteristic of Tcms. Conversely, high glycolytic flux was accompanied by upregulation of transcription factors that regulate terminal effector differentiation, such as Blimp-1, and increased expression of components of the effector machinery, including *Prf1* and *Gzmb*. Our results are consistent with a model whereby elevated glucose metabolism is used by the cell to sustain a global program of effector differentiation that is antagonistic to the molecular circuit regulating memory differentiation.

Whether glucose metabolism directly or indirectly regulates distinct transcriptional factors of Teff versus memory T cell lineages needs further investigation. A recent study from Pearce's group, however, has provided new insights on how metabolic enzymes can directly influence transcription (18). The authors found that the glycolytic enzyme glyceraldehyde-3-phosphate dehydrogenase can bind to the adenylate uridylate–rich elements in the 3′-UTRs of IFN-γ, limiting its translation.

In the current study, we also addressed the metabolic qualities associated with increased effectiveness of adoptively transferred antitumor T cells. Current methods used to produce T cells for adoptive immunotherapy have the pitfall of driving cells toward terminal differentiation and senescence (52, 53). We found that inhibition of glycolysis limited the detrimental influence of ex vivo expansion on T cell differentiation, resulting in the generation of antitumor cells with improved fitness. T cells primed in the presence of 2DG accumulated at higher numbers in tumor deposits and displayed increased proliferative potential and effector function, as measured by enhanced tumor destruction. These findings have important implications for the design of both T cell–based therapies and vaccines for the prevention and treatment of cancer and infectious diseases, since they indicate that pharmacological targeting of metabolic pathways during T cell priming can promote the generation of long-lived CD8⁺ T cell immunity. To this end, reagents that are currently under evaluation in clinical trials because of their direct negative impact on glycolytic tumor cells, including 2DG, might be repurposed to enhance the formation of CD8⁺ T cell memory (54). Thus, modulation of the metabolism of the antitumor T cell response could be an important addition to the immunotherapist's armamentarium.

Methods

Mice and tumor lines. pmel-1 Thy-1.1 (B6.Cg-Thy-1a/Cy Tg [TcraTcrb] 8Rest/J) and C57BL/6 mice were obtained from the Jackson Laboratory. We crossed

pmel-1 with Ly5.1 mice (B6.SJL-Ptprc^a *Pepc*^{b}/BoyJ) to obtain pmel-1 Ly5.1 mice. B16 (H-2D^b), a gp100$^+$ murine melanoma, was obtained from the National Cancer Institute Tumor Repository and maintained in culture media as previously described (4).

In vitro activation of T cells. CD8$^+$ T cells from pmel-1 mice were stimulated in vitro with 1 μM hgp100$_{25–33}$ peptide or plate-bound anti-CD3 (2 μg/ml; 145-2C11; BD Biosciences) and soluble anti-CD28 (1 μg/ml; 37.5 l; BD Biosciences) and expanded in culture medium containing 10 ng·ml^{-1} IL-2 (Chiron) for 4 days. T cells were incubated with 2DG (Sigma-Aldrich) or vehicle (culture media) at indicated doses in the main text and figure legends. CD8$^+$ T cells from C57BL/6 mice were stimulated using plate bound anti-CD3 and soluble anti-CD28 and expanded in culture medium containing 10 ng·ml^{-1} IL-2 (Chiron) for 4 days.

Adoptive cell transfer, infection, recall response, and tumor experiments. Adoptive transfer of purified CD8$^+$ T cells and infection with gp100-VV were performed as previously described (4). Recall response experiments were performed 30 days after primary infection with gp100-VV by rechallenging mice with 10^8 pfu ad-gp100. Tumor experiments were performed using 10^6 activated pmel-1 Thy-1.1 CD8$^+$ T cells as previously described (4).

Cell proliferation assay. We labeled pmel-1 splenocytes with 5 μM Cell proliferation dye eFluor670 (eBioscience), stimulated in vitro with 1 μM hgp100$_{25–33}$ peptide, and expanded in culture medium containing 10 ng·ml^{-1} IL-2 for 4 days. Dilution of Cell proliferation dye was then evaluated by flow cytometry.

Antibodies, flow cytometry, and cell sorting. Mouse antibodies specific for anti-CD8α (53-6.7), anti–Thy-1.1 (OX-7), anti-CD44 (IM7), anti-CD62L (MEL-14), anti-CD25 (PC61), anti-CD27 (LG.3A10), anti–IFN-γ (554413), anti–TNF-α (MP6-XT22), and anti–KLRG-1 (2F1) were from BD Biosciences. Mouse antibody specific for anti-CD69 (H1.2F3) was from eBioscience. FACS Canto I or FACS Canto II (BD Biosciences) was used for flow cytometry acquisition. Samples were analyzed with FlowJo software (Tree-Star). Cells were sorted on the basis of 2-NBDG levels with a FACS Aria instrument (BD Biosciences).

OCR and ECAR. OCR and ECAR were measured at 37°C using an XF24 extracellular analyzer (Seahorse Bioscience) as previously described (22). Briefly, cells were initially plated to unbuffered DMEM (DMEM with 25 mM glucose as indicated, 1 mM sodium pyruvate, 32 mM NaCl, 2 mM GlutaMax, pH 7.4) and incubated in a non-CO_2 incubator for 30 minutes at 37°C. ECAR and OCR were calculated using Seahorse XF-24 proprietary software. In experiments evaluating the acute response to glucose supplementation, we used media with 0 mM glucose and add 25 mM glucose at the indicated time point through the injection port.

Real-time RT-PCR. We isolated RNA with the RNeasy mini kit (Qiagen) and generated cDNA by reverse transcription (Applied Biosystems). Real-time RT-PCR was performed for all genes with primers from Applied Biosystems by Prism 7900HT (Applied Biosystems). Gene expression was calculated relative to *Actb*.

Retroviral vector construction and virus production. Pgam1 cDNA sequence was cloned into retroviral MSCV vector that has GFP as a reporter gene (Addgene 9044). Platinum Eco cell lines (Cell Biolabs) were used for gamma retroviral production by transfection with DNA plasmids through the use of Lipofectamine 2000 (Invitrogen), and virus was collected 48 hours after transfection.

In vitro transduction of CD8$^+$ T cells. Mouse CD8$^+$ T cells were separated from non-CD8$^+$ T cells with a MACS negative selection kit (Miltenyi Biotech) and activated on plates coated with anti-CD3 (2 μg/ml; 145-2C11; BD Biosciences) and soluble anti-CD28 (1 μg/ml; 37.5l; BD Biosciences) in cell culture media containing IL-2 (10 ng/ml; Chiron). Virus were "spin-inoculated" at 2,000 *g* for 2 hours at 32°C onto plates coated with retronectin (Takara). CD8$^+$ T cells were activated for 24 hours and transduced as previously described (33). 72 hours after retroviral transduction, GFP$^+$ cells were sorted with a flow cytometer and used for adoptive transfer experiments.

Immunoblot analysis. Western blot analysis was performed using standard protocols. Proteins were separated by 4%–12% SDS-PAGE, followed by standard immunoblot analysis using anti–Hif1-α (R&D Biosciences), Hk2, p-AMPK, p-Foxo1/3a, total Foxo1, tubulin, and anti–β-actin (Cell Signalling). A 1:1,000 dilution was used for all antibodies.

Cell fractionation and protein analysis. Cytosolic and nuclear fractionation to study the subcellular distribution of Foxo1 were performed as described previously (55).

Enumeration of adoptively transferred cells. We euthanized mice at the indicated time points after infection. Splenocytes were enumerated by trypan blue exclusion. The frequency of transferred T cells was determined by measuring CD8 and Thy-1.1 or GFP with flow cytometry. The absolute number of pmel-1 cells was calculated by multiplying the total cell count by the percent CD8$^+$Thy-1.1$^+$.

Metabolomics. Using a flow cytometer, we purified Tns (CD8$^+$CD44$^-$ CD62L$^+$) and Teffs (CD8$^+$CD44$^+$CD62L$^-$) generated after priming pmel-1 CD8$^+$ T cells with hgp100$_{25–33}$ peptide for 5 days. 6 biological replicates of Tns and Teffs were analyzed. Samples were split for separate analysis on GC/MS and LC/MS/MS platforms (see Supplemental Methods).

Glucose uptake assays. 2 × 10^6 CD8$^+$ T cells were incubated for 10 minutes in 500 μl glucose-free media. 500 μl glucose-free media containing 1 μCi/ml [^{3}H] 2DG (Perkin Elmer) was then added, and cells were incubated for a further 20 minutes. Cells were pelleted, washed in PBS, and then lysed in water. Lysate 3H content was then measured via liquid scintillation counting. For flow cytometry–based glucose uptake assays, we incubated CD8$^+$ T cells with 100 μM 2-NBDG (Invitrogen) for 2 hours before measuring fluorescence by flow cytometry.

Statistics. Data sets were compared using 1- or 2-tailed unpaired Student's *t* test. A log-rank test was used for analysis of survival curves. For all analyses, a *P* value less than 0.05 was considered statistically significant.

Study approval. All animal experiments were conducted with the approval of the National Cancer Institute Animal Use and Care Committee (protocol SB-126).

Acknowledgments

This research was supported by the Intramural Research Program of the NIH, National Cancer Institute, Center for Cancer Research. The authors thank N. Acquavella, D. Clever, E. Tran, and M. Rao for critical review of the manuscript; A. Mixon, S. Farid, and G. Wiegand of the Flow Cytometry Unit for help with cell sorting; and D. Goldstein and M. Malik for catalyzing interactions with Metabolon. We sincerely thank Steven A. Rosenberg for his continuous support.

Received for publication February 27, 2013, and accepted in revised form July 24, 2013.

Address correspondence to: Madhusudhanan Sukumar, Center for Cancer Research, Surgery Branch, National Cancer Institute, NIH, Clinical Research Center, Room 3W-5816, Bethesda, Maryland 20892, USA. Phone: 301.451.0235; Fax: 301.451.6949; E-mail: sukumarm2@mail.nih.gov. Or to: Luca Gattinoni, Center for Cancer Research, Experimental Transplantation and Immunology Branch, National Cancer Institute, NIH, Clinical Research Center, Room 3E-3150, Bethesda, Maryland 20892, USA. Phone: 301.451.6914; Fax: 301.480.4354; E-mail: gattinol@mail.nih.gov.

1. Williams MA, Bevan MJ. Effector and memory CTL differentiation. *Annu Rev Immunol*. 2007;25:171–192.
2. Klebanoff CA, Gattinoni L, Restifo NP. CD8+ T-cell memory in tumor immunology and immunotherapy. *Immunol Rev*. 2006;211:214–224.
3. Gattinoni L, Klebanoff CA, Restifo NP. Paths to stemness: building the ultimate antitumour T cell. *Nat Rev Cancer*. 2012;12(10):671–684.
4. Gattinoni L, et al. Wnt signaling arrests effector T cell differentiation and generates CD8+ memory stem cells. *Nat Med*. 2009;15(7):808–813.
5. Gattinoni L, et al. A human memory T cell subset with stem cell-like properties. *Nat Med*. 2011; 17(10):1290–1297.
6. Wherry EJ, et al. Lineage relationship and protective immunity of memory CD8 T cell subsets. *Nat Immunol*. 2003;4(3):225–234.
7. Thaventhiran JE, Fearon DT, Gattinoni L. Transcriptional regulation of effector and memory CD8 T cell fates. *Curr Opin Immunol*. 2013;25(3):321–328.
8. Kaech SM, Cui W. Transcriptional control of effector and memory CD8+ T cell differentiation. *Nat Rev Immunol*. 2012;12(11):749–761.
9. MacIver NJ, Michalek RD, Rathmell JC. Metabolic regulation of T lymphocytes. *Annu Rev Immunol*. 2013;31:259–283.
10. Michalek RD, Rathmell JC. The metabolic life and times of a T-cell. *Immunol Rev*. 2010;236:190–202.
11. van der Windt GJ, Pearce EL. Metabolic switching and fuel choice during T-cell differentiation and memory development. *Immunol Rev*. 2012;249(1):27–42.
12. Powell JD, Pollizzi K. Fueling memories. *Immunity*. 2012;36(1):3–5.
13. Gerriets VA, Rathmell JC. Metabolic pathways in T cell fate and function. *Trends Immunol*. 2012; 33(4):168–173.
14. Wang R, Green DR. Metabolic checkpoints in activated T cells. *Nat Immunol*. 2012;13(10):907–915.
15. Frauwirth KA, et al. The CD28 signaling pathway regulates glucose metabolism. *Immunity*. 2002;16(6):769–777.
16. Jones RG, Thompson CB. Revving the engine: signal transduction fuels T cell activation. *Immunity*. 2007;27(2):173–178.
17. Wang R, et al. The transcription factor Myc controls metabolic reprogramming upon T lymphocyte activation. *Immunity*. 2011;35(6):871–882.
18. Chang CH, et al. Posttranscriptional control of T cell effector function by aerobic glycolysis. *Cell*. 2013; 153(6):1239–1251.
19. Pearce EL, Pearce EJ. Metabolic pathways in immune cell activation and quiescence. *Immunity*. 2013; 38(4):633–643.
20. Tejera MM, Kim EH, Sullivan JA, Plisch EH, Suresh M. FoxO1 controls effector-to-memory transition and maintenance of functional CD8 T cell memory. *J Immunol*. 2013;191(1):187–199.
21. Pearce EL, et al. Enhancing CD8 T-cell memory by modulating fatty acid metabolism. *Nature*. 2009;460(7251):103–107.
22. van der Windt GJ, et al. Mitochondrial respiratory capacity is a critical regulator of CD8+ T cell memory development. *Immunity*. 2011;36(1):68–78.
23. Araki K, et al. mTOR regulates memory CD8 T-cell differentiation. *Nature*. 2009;460(7251):108–112.
24. Yamada K, Saito M, Matsuoka H, Inagaki N. A real-time method of imaging glucose uptake in single, living mammalian cells. *Nat Protoc*. 2007;2(3):753–762.
25. Zhong L, et al. The histone deacetylase Sirt6 regulates glucose homeostasis via Hif1alpha. *Cell*. 2010;140(2):280–293.
26. Kalia V, Sarkar S, Subramaniam S, Haining WN, Smith KA, Ahmed R. Prolonged interleukin-2Ralpha expression on virus-specific CD8+ T cells favors terminal-effector differentiation in vivo. *Immunity*. 2010;32(1):91–103.
27. Zhou X, Yu S, Zhao DM, Harty JT, Badovinac VP, Xue HH. Differentiation and persistence of memory CD8(+) T cells depend on T cell factor 1. *Immunity*. 2010;33(2):229–240.
28. Jeannet G, Boudousquie C, Gardiol N, Kang J, Huelsken J, Held W. Essential role of the Wnt pathway effector Tcf-1 for the establishment of functional CD8 T cell memory. *Proc Natl Acad Sci U S A*. 2010;107(21):9777–9782.
29. Ichii H, et al. Role for Bcl-6 in the generation and maintenance of memory CD8+ T cells. *Nat Immunol*. 2002;3(6):558–563.
30. Shin H, et al. A role for the transcriptional repressor Blimp-1 in CD8(+) T cell exhaustion during chronic viral infection. *Immunity*. 2009;31(2):309–320.
31. Rutishauser RL, et al. Transcriptional repressor Blimp-1 promotes CD8(+) T cell terminal differentiation and represses the acquisition of central memory T cell properties. *Immunity*. 2009;31(2):296–308.
32. Kallies A, Xin A, Belz GT, Nutt SL. Blimp-1 transcription factor is required for the differentiation of effector CD8(+) T cells and memory responses. *Immunity*. 2009;31(2):283–295.
33. Ji Y, et al. Repression of the DNA-binding inhibitor Id3 by Blimp-1 limits the formation of memory CD8+ T cells. *Nat Immunol*. 2011;12(12):1230–1237.
34. Hallows WC, Yu W, Denu JM. Regulation of glycolytic enzyme phosphoglycerate mutase-1 by Sirt1 protein-mediated deacetylation. *J Biol Chem*. 2012;287(6):3850–3858.
35. Kondoh H, et al. Glycolytic enzymes can modulate cellular life span. *Cancer Res*. 2005;65(1):177–185.
36. Cham CM, Driessens G, O'Keefe JP, Gajewski TF. Glucose deprivation inhibits multiple key gene expression events and effector functions in CD8+ T cells. *Eur J Immunol*. 2008;38(9):2438–2450.
37. Shi LZ, et al. HIF1alpha-dependent glycolytic pathway orchestrates a metabolic checkpoint for the differentiation of TH17 and Treg cells. *J Exp Med*. 2011;208(7):1367–1376.
38. Michalek RD, et al. Cutting edge: distinct glycolytic and lipid oxidative metabolic programs are essential for effector and regulatory CD4+ T cell subsets. *J Immunol*. 2011;186(6):3299–3303.
39. Rolf J, Zarrouk M, Finlay DK, Foretz M, Viollet B, Cantrell DA. AMPKalpha1: A glucose sensor that controls CD8 T-cell memory. *Eur J Immunol*. 2013;43(4):889–896.
40. Finlay DK, et al. PDK1 regulation of mTOR and hypoxia-inducible factor 1 integrate metabolism and migration of CD8+ T cells. *J Exp Med*. 2012; 209(13):2441–2453.
41. Hess MR, Doedens AL, Goldrath AW, Hedrick SM. Differentiation of CD8 memory T cells depends on Foxo1. *J Exp Med*. 2013;210(6):1189–1200.
42. Rao RR, Li Q, Gubbels Bupp MR, Shrikant PA. Transcription factor Foxo1 represses T-bet-mediated effector functions and promotes memory CD8(+) T cell differentiation. *Immunity*. 2012;36(3):374–387.
43. Macintyre AN, et al. Protein kinase B controls transcriptional programs that direct cytotoxic T cell fate but is dispensable for T cell metabolism. *Immunity*. 2011;34(2):224–236.
44. Kerdiles YM, et al. Foxo1 links homing and survival of naive T cells by regulating L-selectin, CCR7 and interleukin 7 receptor. *Nat Immunol*. 2009;10(2):176–184.
45. Finlay D, Cantrell DA. Metabolism, migration and memory in cytotoxic T cells. *Nat Rev Immunol*. 2011; 11(2):109–117.
46. Gattinoni L, et al. Acquisition of full effector function in vitro paradoxically impairs the in vivo antitumor efficacy of adoptively transferred CD8+ T cells. *J Clin Invest*. 2005;115(6):1616–1626.
47. Klebanoff CA, et al. Central memory self/tumor-reactive CD8+ T cells confer superior antitumor immunity compared with effector memory T cells. *Proc Natl Acad Sci U S A*. 2005;102(27):9571–9576.
48. Nolz JC, Harty JT. Protective capacity of memory CD8+ T cells is dictated by antigen exposure history and nature of the infection. *Immunity*. 2011; 34(5):781–793.
49. Muranski P, et al. Th17 cells are long lived and retain a stem cell-like molecular signature. *Immunity*. 2011;35(6):972–985.
50. Rosenberg SA, et al. Durable complete responses in heavily pretreated patients with metastatic melanoma using T-cell transfer immunotherapy. *Clin Cancer Res*. 2011;17(13):4550–4557.
51. Dudda JC, et al. MicroRNA-155 is required for effector CD8+ T cell responses to virus infection and cancer. *Immunity*. 2013;38(4):742–753.
52. Topalian SL, Muul LM, Solomon D, Rosenberg SA. Expansion of human tumor infiltrating lymphocytes for use in immunotherapy trials. *J Immunol Methods*. 1987;102(1):127–141.
53. Riddell SR, Watanabe KS, Goodrich JM, Li CR, Agha ME, Greenberg PD. Restoration of viral immunity in immunodeficient humans by the adoptive transfer of T cell clones. *Science*. 1992;257(5067):238–241.
54. Gattinoni L, Klebanoff CA, Restifo NP. Pharmacologic induction of CD8+ T cell memory: better living through chemistry. *Sci Transl Med*. 2009; 1(11):11ps12.
55. Lal A, Mazan-Mamczarz K, Kawai T, Yang X, Martindale JL, Gorospe M. Concurrent versus individual binding of HuR and AUF1 to common labile target mRNAs. *EMBO J*. 2004;23(15):3092–3102.